Microchemical Journal 187 (2023) 108362

Contents lists available at ScienceDirect

Microchemical Journal

journal homepage: www.elsevier.com/locate/microc

Evaluation of polycrystalline cerium oxide electrodes for electrochemiluminescent detection of sarcosine

Hengameh Bahrami [a], Yuliia Kosto [b,1], Claudio Ignazio Santo [c], Yurii Yakovlev [b], Ivan Khalakhan [b], Mehdi Mousavi [a], Vladimir Matolin [b], Iva Matolinová [b], Francesco Paolucci [c], Giovanni Valenti [c], Nataliya Tsud [b,*], Alessandra Zanut [c,*,2]

[a] Shahid Bahonar University of Kerman, Faculty of Sciences, Department of Chemistry, 76169-14111 Kerman, Iran
[b] Charles University, Faculty of Mathematics and Physics, Department of Surface and Plasma Science, V Holešovičkách 2, 18000 Prague, Czech Republic
[c] University of Bologna, Department of Chemistry, F. Selmi 2, 40126 Bologna, Italy

A B S T R A C T

Prostate cancer (PCa) is widely spread in male population, especially over 65 years. Currently used medical methods of PCa diagnosis often lead to false-positive results thus new non-invasive methods for PCa detection, such as urine tests for cancer metabolites, are actively studied. Herein, nanostructured polycrystalline cerium oxide thin films (CeO_2/GC) prepared by magnetron sputtering on a glassy carbon substrate are tested for electrochemiluminescent (ECL) detection of sarcosine exploiting the oxidative-reduction mechanism using $Ru(bpy)_3^{2+}$ as luminophore. Non-functionalized CeO_2/GC electrodes revealed a higher ECL signal stability compared to bare glassy carbon electrodes. Moreover, CeO_2/GC electrodes were successfully applied for rapid and sensitive detection of different sarcosine concentrations ranging from 50 to 5000 μM. These results open new possibilities for developing sensing platforms for sarcosine detection based on the CeO_2/GC working electrode via surface modification and functionalization, aiming to further investigate and improve their sensitivity and selectivity.

1. Introduction

According to World Health Organization, prostate cancer (PCa) is the fourth most occurred cancer overall and the second in men part of the Earth human population [1]. Actual common screening procedures for PCa include prostate-specific antigen (PSA) blood testing and digital rectal examination (DRE) [2]. However, PSA test may often lead to false-positive results as increased PSA concentration may occur also in benign prostatic hyperplasia or prostatitis. Moreover, DRE is an invasive and uncomfortable procedure with limited sensitivity and specificity [3]. In order to reduce medical expenses and improve patients' quality of life, non-invasive diagnostic methods with high precision, able to detect alternative and more accurate biomarkers for PCa diagnosis are needed [2]. In the last decades, non-invasive urine tests for cancer metabolites became a promising direction for PCa screening. In particular, the monopeptide sarcosine (SA) has been recently studied as a potential biomarker molecule in PCa as its urine concentration increases during cancer progression [4,5]. SA is an *N*-methyl glycine metabolite and it is involved in methylation processes, occurring during the progression of prostate cancer, and in the metabolism of amino acids [6].

SA detection is nowadays performed through standard analytical methods, such as high-performance liquid-chromatography-mass-spectrometry (HPLC/MS) and gas-chromatography-mass-spectrometry (GC/MS), which ensure high sensitivity (in range of nM), but need expensive instrumentation and are time-consuming [7]. In recent years, many research groups have focused on the design and development of biosensing platforms for rapid and easy SA detection, exploiting mainly fluorescent [8–10], luminescent [11], and electrochemical [12,13] schemes. However, determination of SA in urine samples is challenging because it requires high sensitivity toward SA molecules to discriminate it from the rest of the organic matrix.

In this context, electrochemiluminescence (ECL) is an efficient analytical technique widely employed for the development of biosensing platforms for biomarkers detection [14,15]. In the ECL luminescence process the excited states of luminophores are electrochemically generated in proximity of the electrode surface and then relax to a lower state emitting light [16–18]. Thanks to its temporal and spatial control of light emission, ECL possess high sensitivity, wide dynamic range, and

* Corresponding authors.
E-mail addresses: tsud@mbox.troja.mff.cuni.cz (N. Tsud), alessandra.zanut@unipd.it (A. Zanut).
[1] Present address: Brandenburg University of Technology Cottbus-Senftenberg, Applied Physics & Semiconductor Spectroscopy, Konrad-Zuse Str 1, D-03046 Cottbus, Germany.
[2] Present address: University of Padova, Department of Chemical Sciences, F. Marzolo 1, 35131 Padova, Italy.

https://doi.org/10.1016/j.microc.2022.108362
Received 4 July 2022; Received in revised form 23 December 2022; Accepted 26 December 2022
Available online 28 December 2022

good stability even in complex matrixes [14,19,20]. The most efficient ECL scheme for (bio)analytical applications involves the use of ruthenium(II)tris(2.2'-bipyridine) complex $[Ru(bpy)_3]^{2+}$ as luminophore and tri-*n*-propylamine (TPrA) as co-reactant [17,21]. In general, tertiary amines are the most used because they provide the highest ECL intensity and have the lowest limit of detection (LOD) [22,23].

Since SA is a secondary amine, it can also be potentially used in the ECL systems interacting with $Ru(bpy)_3^{2+}$ and assisting in light emission. Indeed, it has been shown that SA acts as a good ECL co-reactant using a supramolecular approach to create a sensor for SA determination in urine samples, providing good selectivity in a concentration range used for medical diagnosis of PCa [24].

It is well known that the ECL efficiency is highly dependent on the electrochemical properties of electrode materials and many strategies have been proposed so far to make suitable electrodes and construct elaborate interfaces [25]. A good electrode material should be stable for extended use, while maintaining good kinetics for co-reactant oxidation. In this context, carbon-based materials, noble materials, and doped materials such as boron-doped diamond possess high chemical stability and high conductivity [26,27]. However, almost all these materials are characterized by scarce porosity plus modification of such electrodes can strongly influence the ECL signal [28].

Among materials, cerium oxide is one of the most promising for biological sensing devices thanks to its catalytic activity, good biocompatibility, oxygen storage capacity, and electron transfer capability [29–31].

Recently, we reported the use of compact polycrystalline cerium oxide thin film deposited on a glassy carbon substrate (CeO_2/GC) as electrode for the electrochemical detection of hydrogen peroxide [32]. Herein, we explore the capability of non-functionalized polycrystalline CeO_2/GC oxide film as a working electrode for ECL generation through an "oxidative-reduction" based scheme using SA as a co-reactant. The ECL detection of SA in aqueous solution (PBS, pH 7.2) was tested and compared with the one at bare glassy carbon electrodes, demonstrating advantages of nanostructured film over flat surfaces. Moreover, polycrystalline CeO_2/GC electrodes demonstrated the ability to distinguish different concentrations of SA in a range suitable for analytical purposes.

2. Experimental

2.1. Materials

All chemicals were of analytical grade and were purchased from Sigma-Aldrich (St. Louis, MO) unless otherwise indicated. Glassy carbon substrates (>99.9 %, 1 mm thick, type 2) were purchased from Alfa Aesar (USA). The phosphate buffer solution (PBS, pH 7.2) was prepared by dissolving 15.9 g of NaH_2PO_4 and 13.9 g of Na_2HPO_4 in 1000 mL of ultrapure water (18 MΩ cm). Total concentration of PBS was 200 mM. SA solutions (0 – 5000 μM) were prepared in PBS 200 mM (pH 7.2) and stored at 4 °C.

2.2. Polycrystalline cerium oxide fabrication and characterization

Polycrystalline cerium oxide films were deposited onto glassy carbon substrate by non-reactive magnetron sputtering of a CeO_2 target (99.999 %, Kurt J. Lesker) under Ar atmosphere (4×10^{-3} mbar). The magnetron sputtering was done using a RF power of 65 W, providing 1 nm min^{-1} growth rate of cerium oxide film. The thickness of the oxide films was estimated to be about 15 nm. The surface morphology and structure were characterized by a Bruker MultiMode 8 atomic force microscope (AFM) and a Tescan Mira 3 scanning electron microscope (SEM).

The chemical state of the CeO_2/GC electrode on the surface and throughout the whole thickness was examined by means of X-ray photoelectron spectroscopy (XPS) technique. The Ce 3d core level spectrum was recorded by XPS, providing information about oxidative state of Ce cations from about 7 nm deep layers of the film. The XPS experiment was conducted at the Materials Science beamline at Elettra synchrotron in Trieste, Italy.

2.3. Electrochemiluminescent detection of SA

ECL and electrochemical (EC) measurements were carried out with an AUTOLAB electrochemical station (Ecochemie, Mod. PGSTAT 30) in a home-made transparent three electrode cell with Ag/AgCl used as reference electrode, a platinum wire as counter electrode, and bare GC or CeO_2/GC as working electrode. During the EC measurements, the surface of CeO_2/GC electrodes in contact with the working solution was delimited by 0.5 cm^2 (circle of 0.8 cm diameter) o-ring. ECL signals were generated in chronoamperometry (CA) mode at potential of 1.4 V and measured with a photomultiplier tube (Acton PMT PD471, Hamamatsu R4220p) placed at a constant distance in front of the cell and inside a dark box. A voltage of 750 V was supplied to the PMT. The light/current/voltage curves were recorded by collecting the pre-amplified PMT output signal (using an ultralow-noise Acton research model 181) with the second input channel of an ADC module of the AUTOLAB instrument.

3. Results and discussion

The structure and morphology of polycrystalline CeO_2/GC electrodes were characterized using SEM and AFM microscopies (Fig. 1a-b). From Fig. 1a the surface mean roughness was estimated to be 1.2–1.3 nm and the grain size between 10 and 30 nm. The obtained XPS results showed a minor contribution of the Ce^{3+} cations within the measured thickness range in the as-prepared samples (Fig. 1c).

CV experiments to evaluate the electrocatalytic behaviour of CeO_2/GC and bare GC working electrodes, were conducted in pure 200 mM PBS solution and in the presence of 1 mM potassium ferricyanide (Fig. S1), confirming good conductivity of the CeO_2/GC substrate. Our group previously investigated the electrochemical properties of CeO_2/GC electrodes in the same conditions, observing good conductibility and larger electro-active area compared to bare GC [32]. Moreover, it was proved that the higher total surface area of the electrode, modified by polycrystalline ceria film, brings to an improved reaction rate for heterogeneous catalysts and the electrode transfer kinetics compared to bare GC electrodes [32].

ECL efficiency of the CeO_2/GC electrode was first tested using $Ru(bpy)_3^{2+}$ as luminophore and TPrA as co-reactant, applying a potential from 0 to 1.4 V vs Ag/AgCl to ensure oxidation of both species [33]. The CV of CeO_2/GC and bare GC (Fig. 2) shows a higher current density of the $Ru(bpy)_3^{2+}$ oxidation peak on the CeO_2/GC electrode compared to the bare GC electrode. Good conductivity of the CeO_2 thin film gives the ability to act as a conducting agent between the $Ru(bpy)_3^{2+}$ and the GC substrate surface, facilitating electron-transfer in the ECL reaction. It was already demonstrated that surface modification of the working electrode by inorganic thin films or nanomaterials, polymer coatings, etc. can increase intensity of the ECL response [17]. These results confirm the compatibility of CeO_2/GC electrodes with the $Ru(bpy)_3^{2+}$/TPrA co-reactant ECL system.

As previously mentioned, tertiary amines are the most productive co-reactants in combination with $Ru(bpy)_3^{2+}$ complex for the generation of ECL signals. However, secondary amines (where the amino group is directly bonded to two carbon atoms of any hybridization), such as SA, have the potential to provide sufficient effectivity for light generation and thus to be used as a co-reactant in ECL experiments. Indeed, SA shows an irreversible oxidation peak at 1 V satisfying the energy requirements for generating the excited state of the chromophore [24]. In this work, the ability of SA to act as a co-reactant for ECL generation has been tested according to the "oxidative-reduction" mechanism in 200 mM PBS using 10 μM $Ru(bpy)_3^{2+}$ on the CeO_2/GC electrode. Fig. 3a shows the ECL signals generated at the CeO_2/GC electrode before and

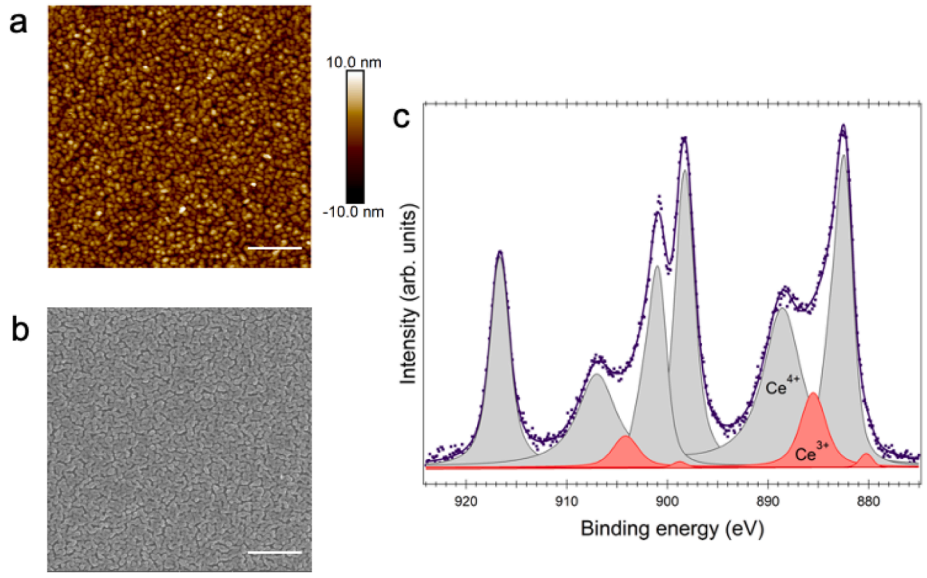

Fig. 1. Polycrystalline CeO_2/GC electrodes characterization. a) AFM and b) SEM images of the 15 nm thick CeO_2/GC thin film. Scale bar 200 nm. c) Ce 3d XPS spectrum taken from the as-prepared oxide film with photon energy 1486.6 eV. Violet dots and solid line correspond to the measured data and fit result, respectively. Gray peaks are attributed to the Ce^{4+} cations, and red peaks to the Ce^{3+} cations. (For interpretation of the references to colour in this figure legend, the reader is referred to the web version of this article.)

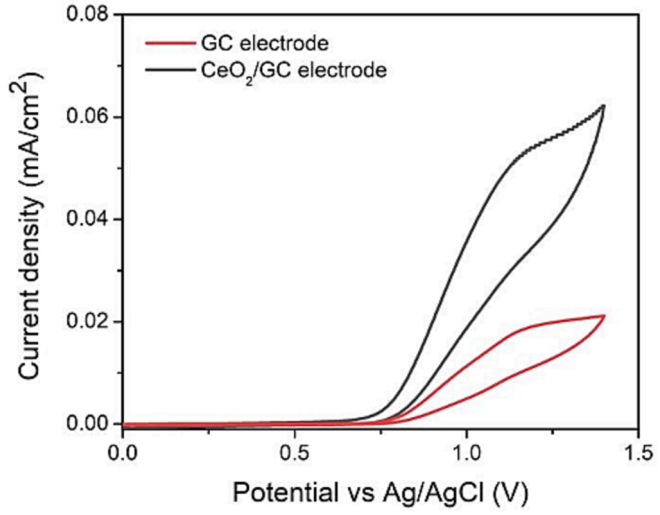

Fig. 2. Cyclic voltammogram of GC (red) and CeO_2/GC (black) electrode recorded in 200 mM PBS (pH 7.2) containing 30 mM TPrA and 10 μM Ru $(bpy)_3^{2+}$. Scan rate of 100 mV/s, potential range from 0 to 1.4 V. (For interpretation of the references to colour in this figure legend, the reader is referred to the web version of this article.)

after the addition of 5 mM SA as co-reactant.

The proposed mechanism for ECL generation involves the reaction between SA and $Ru(bpy)_3^{2+}$ to form the excited state $Ru(bpy)_3^{2+*}$, which relaxes to the ground state generating light. The reaction can be described as follow:

$$Ru(bpy)_3^{2+} - e^- \rightleftarrows Ru(bpy)_3^{3+} \quad (1)$$

$$R\text{-}NHCH_3 - e^- \rightleftarrows R\text{-}NHCH_3^+ \quad (2)$$

$$R\text{-}NHCH_3^+ \rightleftarrows R\text{-}NHCH_3^{\bullet} + H^+ \quad (3)$$

$$Ru(bpy)_3^{3+} + R\text{-}NHCH_3^{\bullet} \rightleftarrows Ru(bpy)_3^{2+*} \quad (4)$$

$$Ru(bpy)_3^{2+*} \rightleftarrows Ru(bpy)_3^{2+} + h\nu \quad (5)$$

To evaluate the sensing ability of the CeO_2/GC electrode to different concentrations of SA, the experiment was conducted in 10 μM $Ru(bpy)_3^{2+}$ PBS solution with stepwise addition of SA (50–5000 μM) (Fig. 3b). Concentrations of sarcosine were chosen to investigate a wide range of values useful for analytical applications.

Inset of Fig. 3b shows the maximum ECL intensity profile at different concentrations of sarcosine in the working solution (hereinafter called calibration curve) taken with CeO_2/GC electrodes. For comparison and estimation of the CeO_2/GC electrode efficiency, the same measurements were repeated with the bare GC electrode (Fig. S2). The results reveal a direct dose–response correlation between the sarcosine concentration and the ECL signal intensity.

The LOD parameter was calculated from the obtained calibration lines (Fig. S3) using the following formula:

$$LOD = \frac{(K \times S_b)}{m}$$

where K equals 3 (confidence level 98.3 %), S_b is the standard deviation of the blank solution, and m is the calibration sensitivity (slope of the calibration curve). Under the optimized experimental conditions, the LOD was found to be 45.9 and 63.10 μM for CeO_2/GC and bare GC electrodes, respectively. It confirms that GC electrodes modified with polycrystalline cerium oxide thin film is able to detect low concentrations of SA.

It is worth noting that on the CeO_2/GC electrode the intensity, measured as the total area under the ECL peak, is higher than on the bare GC (Fig. 4), suggesting that the polycrystalline CeO_2/GC electrode possesses better electroanalytical performance and electrochemical stability. This response may be ascribed to enzymatic-like activity of polycrystalline cerium oxide [32,34,35], particularly visible at higher SA concentration where SA interacts with the electrode surface at faster rates. In addition, thanks to its higher surface area, CeO_2 modified electrode saturates at higher concentration of analytes.

This represents another advantage of CeO_2/GC electrodes over bare GC ones, on which the oxygen-containing surface species, which decrease the efficiency of coreactant oxidation, are usually formed [20,36,37].

To evaluate the effect of possible interferents on ECL signals, we tested three representative Sarcosine concentrations (0, 50, 3000 μM) using CeO_2/GC electrodes in a solution of 10 μM $Ru(bpy)_3^{2+}$ containing BSA 10 mg/ml which mimic the concentration present in human urine (Fig. S4a). Obtained results confirm the ability of CeO_2/GC electrodes to discriminate between different SA concentrations even in presence of

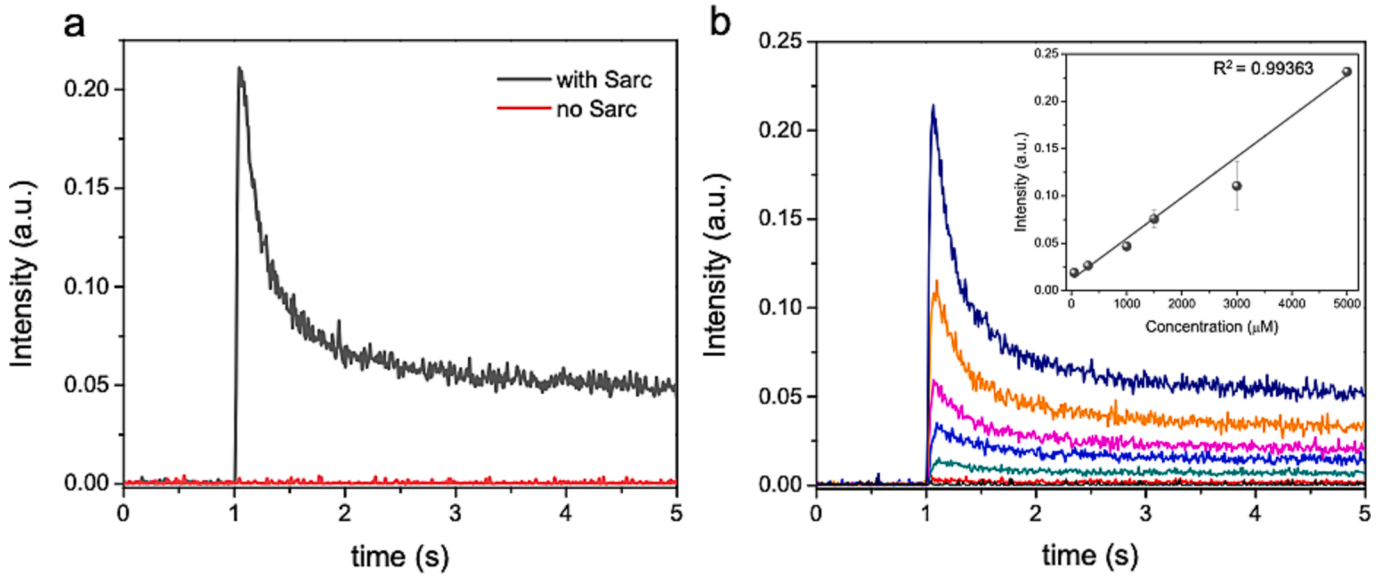

Fig. 3. ECL generation using sarcosine as a co-reactant. ECL signal recorded in chronoamperometry mode using CeO_2/GC electrodes measured at 1.4 V in 200 mM PBS (pH 7.2) containing 10 μM $Ru(bpy)_3^{2+}$ **a)** with (black) and without (red) 5 mM SA as co-reactant and **b)** after addition of 50 (red), 300 (green), 1000 (blue), 1500 (pink), 3000 (orange), and 5000 μM (dark blue) of sarcosine. Inset shows the max ECL value as a function of SA concentration. The error is represented as the standard deviation (n = 3) and is equal to 0.00065. (For interpretation of the references to colour in this figure legend, the reader is referred to the web version of this article.)

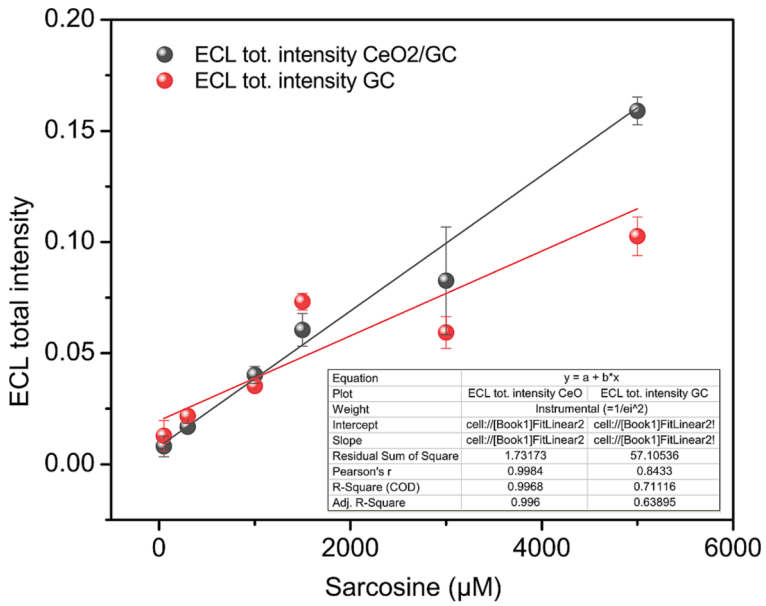

Fig. 4. The ECL total intensity as a function of sarcosine concentration is measured on bare GC and CeO_2/GC electrodes in 200 mM PBS (pH 7.2) containing 10 μM $Ru(bpy)_3^{2+}$. The error is represented as standard deviation (n = 3).

BSA 10 mg/ml. Moreover, signals are reproducible as confirmed by the calculated RSD% which is ≤ 5 % for both concentrations (Fig. S4b).

4. Conclusions

Polycrystalline cerium oxide thin films prepared by magnetron sputtering on glassy carbon substrate were studied as electrodes for ECL detection of sarcosine, using SA as a co-reactant in oxidative-reduction mechanism with $Ru(bpy)_3^{2+}$ as luminophore. Obtained results revealed that modification of the bare glassy carbon electrode by polycrystalline cerium oxide layers increases the electrode's electroactive area and enhances its catalytic properties. Moreover, the comparative study with bare glassy carbon electrodes revealed a higher ECL stability on the CeO_2/GC electrode due to its higher surface area. The CeO_2/GC electrode was successfully applied for rapid and sensitive detection of different SA concentrations (50 – 5000 μM). CeO_2/GC was shown to be a more efficient electrode material for ECL applications compared to the commercial GC electrode. LOD of the CeO_2/GC electrode was estimated to be 45.9 μM which makes it suitable for SA detection in the concentration range used in clinical assays for PCa diagnostics. Preliminary results demonstrated the ability of CeO_2/GC electrodes to detect low concentration of SA also in presence of BSA 10 mg/ml with a good reproducibility (RSD ≤ 5 %). Further investigations are ongoing in our laboratories to better assess the analytical strength of this system in complex matrices (i.e. urine). These results open new possibilities for the development of sensors for SA detection based on the CeO_2/GC working

electrode via surface modification and functionalization, with the aim to further investigate and improve their sensitivity and selectivity.

CRediT authorship contribution statement

Hengameh Bahrami: Investigation, Formal analysis, Data curation. **Yuliia Kosto:** Investigation, Formal analysis, Visualization. **Claudio Ignazio Santo:** Investigation, Validation. **Yurii Yakovlev:** Resources, Writing – review & editing. **Ivan Khalakhan:** Resources, Writing – review & editing. **Mehdi Mousavi:** Writing – review & editing. **Vladimir Matolin:** Writing – review & editing. **Iva Matolinová:** Writing – review & editing, Funding acquisition. **Francesco Paolucci:** Writing – review & editing, Funding acquisition. **Giovanni Valenti:** Supervision, Conceptualization, Writing – review & editing. **Nataliya Tsud:** Supervision, Writing – review & editing. **Alessandra Zanut:** Conceptualization, Methodology, Visualization, Writing – original draft.

Declaration of Competing Interest

The authors declare that they have no known competing financial interests or personal relationships that could have appeared to influence the work reported in this paper.

Data availability

Data will be made available on request.

Acknowledgement

The CERIC-ERIC consortium and the Czech Ministry of Education, Youth and Sports (project LM2018116) are acknowledged for financial support. This work is supported by the Italian Ministero dell'Istruzione, Università e Ricerca (PRIN-2017FJCPEX) and University of Bologna and Fondazione CarisBo (project #18668).

Appendix A. Supplementary data

Supplementary data to this article can be found online at https://doi.org/10.1016/j.microc.2022.108362.

References

[1] World Cancer Research Fund International https://www.wcrf.org/cancer-trends/prostate-cancer-statistics/.
[2] K.M. Chan, J.M. Gleadle, M. O'Callaghan, K. Vasilev, M. MacGregor, Prostate Cancer Detection: A Systematic Review of Urinary Biosensors, Prostate Cancer Prostatic Dis. No. August (2022) 1–8, https://doi.org/10.1038/s41391-021-00480-8.
[3] L. Klotz, Prostate Cancer Overdiagnosis and Overtreatment, Curr. Opin. Endocrinol. Diabetes Obes. 20 (3) (2013) 204–209, https://doi.org/10.1097/MED.0b013e328360332a.
[4] A. Sreekumar, L.M. Poisson, T.M. Rajendiran, A.P. Khan, Q. Cao, J. Yu, B. Laxman, R. Mehra, R.J. Lonigro, Y. Li, M.K. Nyati, A. Ahsan, S. Kalyana-Sundaram, B. Han, X. Cao, J. Byun, G.S. Omenn, D. Ghosh, S. Pennathur, D.C. Alexander, A. Berger, J. R. Shuster, J.T. Wei, S. Varambally, C. Beecher, A.M. Chinnaiyan, Metabolomic Profiles Delineate Potential Role for Sarcosine in Prostate Cancer Progression, Nature 457 (7231) (2009) 910–914, https://doi.org/10.1038/nature07762.
[5] J. Couzin, BIOMARKERS: Metabolite in Urine May Point To High-Risk Prostate Cancer, 865a 865a, Science. 323 (5916) (2009), https://doi.org/10.1126/science.323.5916.865a.
[6] P. Dereziński, A. Klupczynska, W. Sawicki, J.A. Pałka, Z.J. Kokot, Amino Acid Profiles of Serum and Urine in Search for Prostate Cancer Biomarkers: A Pilot Study, Int. J. Med. Sci. 14 (1) (2017) 1–12, https://doi.org/10.7150/ijms.15783.
[7] Y. Jiang, X. Cheng, C. Wang, Y. Ma, Quantitative Determination of Sarcosine and Related Compounds in Urinary Samples by Liquid Chromatography with Tandem Mass Spectrometry, Anal. Chem. 82 (21) (2010) 9022–9027, https://doi.org/10.1021/ac1019914.
[8] E. Biavardi, C. Tudisco, F. Maffei, A. Motta, C. Massera, G.G. Condorelli, E. Dalcanale, Exclusive Recognition of Sarcosine in Water and Urine by a Cavitand-Functionalized Silicon Surface, Proc. Natl. Acad. Sci. 109 (7) (2012) 2263–2268, https://doi.org/10.1073/pnas.1112264109.
[9] Y. Luo, J. Wang, L. Yang, T. Gao, R. Pei, Sensors and Actuators B : Chemical In Vitro Selection of DNA Aptamers for the Development of Fl Uorescent Aptasensor for Sarcosine Detection, Sensors Actuators B. Chem. 276 (April) (2018) 128–135, https://doi.org/10.1016/j.snb.2018.08.105.
[10] W. Li, T. Li, S. Chen, D. Deng, Y. Ji, R. Li, Sensors and Actuators : B. Chemical Nanozyme-Mediated Cascade Reaction System for Ratiometric Fluorescence Detection of Sarcosine, Sensors Actuators B. Chem. October 2021 (355) (2022), 131341, https://doi.org/10.1016/j.snb.2021.131341.
[11] L. Zhao, J. Yang, M. Gong, K.e. Li, J. Gu, Specific Screening of Prostate Cancer Individuals Using an Enzyme-Assisted Substrate Sensing Platform Based on Hierarchical MOFs with Tunable Mesopore Size, J. Am. Chem. Soc. 143 (37) (2021) 15145–15151.
[12] J. Hu, W. Wei, S. Ke, X. Zeng, P. Lin, Electrochimica Acta A Novel and Sensitive Sarcosine Biosensor Based on Organic Electrochemical Transistor, Electrochim. Acta 307 (2019) 100–106, https://doi.org/10.1016/j.electacta.2019.03.180.
[13] T. Liu, B.o. Fu, J. Chen, K. Li, An electrochemical sarcosine sensor based on biomimetic recognition, Microchim Acta 186 (3) (2019).
[14] Faatz, E.; Finke, A.; Josel, H. P.; Prencipe, G.; Quint, S.; Windfuhr, M. Chapter 15: Automated Immunoassays for the Detection of Biomarkers in Body Fluids. *RSC Detect. Sci.* **2020**, *2020-January* (15), 443–470. doi: 10.1039/9781788015776-00443.
[15] A. Zanut, A. Fiorani, S. Canola, T. Saito, N. Ziebart, S. Rapino, S. Rebeccani, A. Barbon, T. Irie, H.-P. Josel, F. Negri, M. Marcaccio, M. Windfuhr, K. Imai, G. Valenti, F. Paolucci, Insights into the Mechanism of Coreactant Electrochemiluminescence Facilitating Enhanced Bioanalytical Performance, Nat. Commun. 11 (1) (2020) 2668, https://doi.org/10.1038/s41467-020-16476-2.
[16] Bouffier, L.; Sojic, N. Chapter 1: Introduction and Overview of Electrogenerated Chemiluminescence. *RSC Detect. Sci.* **2020**, *2020-Janua* (15), 1–28. doi: 10.1039/9781788015776-00001.
[17] J.R. Forster, P. Bertoncello, K.E. Tia, Electrogenerated Chemiluminescence, Annu. Rev. Anal. Chem. 2 (2009) 359–385, https://doi.org/10.1146/annurev-anchem-060908-155305.
[18] M.M. Richter, Electrochemiluminescence (ECL), Chem. Rev. 104 (2004) 3003–3036, https://doi.org/10.1021/cr020373d.
[19] J. Zhang, S. Arbault, N. Sojic, D. Jiang, Electrochemiluminescence Imaging for Bioanalysis, Annu. Rev. Anal. Chem. 12 (1) (2019) 275–295, https://doi.org/10.1146/annurev-anchem-061318-115226.
[20] S. Rebeccani, A. Zanut, C.I. Santo, G. Valenti, F. Paolucci, A Guide Inside Electrochemiluminescent Microscopy Mechanisms for Analytical Performance Improvement, Anal. Chem. 94 (1) (2022) 336–348, https://doi.org/10.1021/acs.analchem.1c05065.
[21] E. Kerr, E.H. Doeven, G.J. Barbante, C.F. Hogan, D.J. Bower, P.S. Donnelly, T. U. Connell, P.S. Francis, Annihilation Electrogenerated Chemiluminescence of Mixed Metal Chelates in Solution: Modulating Emission Colour by Manipulating the Energetics, Chem. Sci. 6 (1) (2015) 472–479, https://doi.org/10.1039/C4SC02697G.
[22] X. Liu, L. Shi, W. Niu, H. Li, G. Xu, Environmentally Friendly and Highly Sensitive Ruthenium(II) Tris(2,2′-Bipyridyl) Electrochemiluminescent System Using 2-(Dibutylamino)Ethanol as Co-Reactant, Angew. Chem. Int. Ed. 46 (3) (2007) 421–424, https://doi.org/10.1002/anie.200603491.
[23] Y. Yuan, S. Han, L. Hu, S. Parveen, G. Xu, Coreactants of Tris(2,2′-Bipyridyl) Ruthenium(II) Electrogenerated Chemiluminescence, Electrochim. Acta 82 (2012) 484–492, https://doi.org/10.1016/j.electacta.2012.03.156.
[24] G. Valenti, E. Rampazzo, E. Biavardi, E. Villani, G. Fracasso, M. Marcaccio, F. Bertani, D. Ramarli, E. Dalcanale, F. Paolucci, L. Prodi, An Electrochemiluminescence-Supramolecular Approach to Sarcosine Detection for Early Diagnosis of Prostate Cancer, Faraday Discuss. 185 (2015) 299–309, https://doi.org/10.1039/C5FD00096C.
[25] G. Valenti, A. Fiorani, H. Li, N. Sojic, F. Paolucci, Essential Role of Electrode Materials in Electrochemiluminescence Applications, ChemElectroChem 3 (12) (2016) 1990–1997.
[26] A. Fiorani, J.P. Merino, A. Zanut, A. Criado, G. Valenti, M. Prato, F. Paolucci, Advanced Carbon Nanomaterials for Electrochemiluminescent Biosensor Applications, Current Opinion in Electrochemistry. 16 (2019) 66–74.
[27] K. Sakanoue, A. Fiorani, C.I. Santo, Irkham, G. Valenti, F. Paolucci, Y. Einaga, Boron-Doped Diamond Electrode Outperforms the State-of-the-Art Electrochemiluminescence from Microbeads Immunoassay, ACS Sensors 7 (4) (2022) 1145–1155.
[28] P. Nikolaou, G. Valenti, F. Paolucci, Nano-Structured Materials for the Electrochemiluminescence Signal Enhancement, Electrochim. Acta 388 (2021), 138586, https://doi.org/10.1016/j.electacta.2021.138586.
[29] A. Karimi, S.W. Husain, M. Hosseini, P.A. Azar, M.R. Ganjali, Rapid and Sensitive Detection of Hydrogen Peroxide in Milk by Enzyme-Free Electrochemiluminescence Sensor Based on a Polypyrrole-Cerium Oxide Nanocomposite, Sensors Actuators, B Chem. 271 (January) (2018) 90–96, https://doi.org/10.1016/j.snb.2018.05.066.
[30] G. Valenti, M. Melchionna, T. Montini, A. Boni, L. Nasi, E. Fonda, A. Criado, A. Zitolo, S. Voci, G. Bertoni, M. Bonchio, P. Fornasiero, F. Paolucci, M. Prato, Water-Mediated ElectroHydrogenation of CO2 at Near-Equilibrium Potential by Carbon Nanotubes/Cerium Dioxide Nanohybrids, ACS Appl. Energy Mater. 3 (9) (2020) 8509–8518, https://doi.org/10.1021/acsaem.0c01145.
[31] N. Alizadeh, A. Salimi, T.-K. Sham, P. Bazylewski, G. Fanchini, Intrinsic Enzyme-like Activities of Cerium Oxide Nanocomposite and Its Application for Extracellular H2O2 Detection Using an Electrochemical Microfluidic Device, ACS Omega 5 (21) (2020) 11883–11894, https://doi.org/10.1021/acsomega.9b03252.
[32] Y. Kosto, A. Zanut, S. Franchi, Y. Yakovlev, I. Khalakhan, V. Matolín, K.C. Prince, G. Valenti, F. Paolucci, N. Tsud, Electrochemical Activity of the Polycrystalline

Cerium Oxide Films for Hydrogen Peroxide Detection, Appl. Surf. Sci. 488 (2019) 351–359, https://doi.org/10.1016/j.apsusc.2019.05.205.
[33] W. Miao, J.-P. Choi, A.J. Bard, Electrogenerated Chemiluminescence 69: The Tris (2,2'-Bipyridine)Ruthenium(II), (Ru(Bpy) 3 2+)/Tri- n -Propylamine (TPrA) System RevisitedA New Route Involving TPrA •+ Cation Radicals, J. Am. Chem. Soc. 124 (48) (2002) 14478–14485, https://doi.org/10.1021/ja027532v.
[34] Y.N. Khonsari, S. Sun, A novel MIP-ECL sensor based on RGO–CeO2NP/Ru(bpy)32 +-chitosan for ultratrace determination of trimipramine, Journal of Materials Chemistry B 9 (2021) 471–478, https://doi.org/10.1039/D0TB01666G.
[35] M. Li, J. Fang, C. Wang, J. Zhang, L. Liu, Y. Li, W. Cao, Q. Wei, CePO4/CeO2 heterostructure and enzymatic action of D-Fe2O3 co-amplify luminol-based electrochemiluminescence immunosensor for NSE detection, Biosens. Bioelectron. 214 (2022), 114516, https://doi.org/10.1016/j.bios.2022.114516.
[36] P. Dutta, D. Han, B. Goudeau, D. Jiang, D. Fang, N. Sojic, Reactivity Mapping of Luminescence in Space: Insights into Heterogeneous Electrochemiluminescence Bioassays, Biosens. Bioelectron. 165 (May) (2020), 112372, https://doi.org/10.1016/j.bios.2020.112372.
[37] D. Han, B. Goudeau, D. Jiang, D. Fang, N. Sojic, Electrochemiluminescence Microscopy of Cells: Essential Role of Surface Regeneration, Anal. Chem. 93 (3) (2021) 1652–1657, https://doi.org/10.1021/acs.analchem.0c05123.